Formation Mechanisms for Convection over the Ligurian Sea during MAP IOP-8

YUH-LANG LIN, HEATHER DAWN REEVES, SHU-YUN CHEN, AND SEN CHIAO

Department of Marine, Earth, and Atmospheric Sciences, North Carolina State University, Raleigh, North Carolina

(Manuscript received 1 June 2004, in final form 5 January 2005)

ABSTRACT

The dynamical impacts of an unusually strong stable layer that developed over the Po Valley and northern Ligurian Sea during Mesoscale Alpine Program (MAP) intensive observation period 8 (IOP-8) on the formation of convection over the Ligurian Sea are explored. Based on numerically simulated equivalent potential temperature, wind vectors, and by a trajectory analysis of parcels both beneath and above the stable layer, it is shown that the stable layer behaved as a material surface or "effective mountain" to the airstreams impinging on it from the south. Additional analyses show that the leading edge of the stable layer was collocated with maxima in upward motion and a strong positive moisture flux. Hence, it was further argued and demonstrated through inspection of soundings upstream of the cold dome and trajectory analyses that lifting by the stable layer enhanced convective activities over the Ligurian Sea. Finally, processes contributing to the maintenance of the stable layer during IOP-8 were explored. It was found that the differential advection of a warm, less stable air mass on top of a cooler, more stable air mass helped maintain the stable layer. The Ligurian Apennines made a secondary contribution to the stagnation of the cool air in the Po Valley by partially blocking this air mass from exiting the valley to the south.

1. Introduction

One of the major objectives of the Mesoscale Alpine Program (MAP) is to understand the dynamics and improve the prediction of heavy orographic precipitation (Binder and Schär 1996; Bougeault et al. 2001). This component of the field experiment is also known as Wet MAP. Among the Wet MAP intensive observation periods (IOPs), IOP-8 has garnered much attention from the MAP scientific community. The reason for such interest is that the synoptic environment of this event had many ingredients common in heavy orographic precipitation events (Lin et al. 2001; Medina and Houze 2003; Rotunno and Ferretti 2003). In fact, both the Swiss Model and the Mesoscale Compressible Community model, as well as some experienced forecasters, predicted heavy precipitation over the Lago Maggiore target area (LMTA; see Fig. 1), which is located in the concave region of the arc-shaped Alps (Bousquet and Smull 2003, hereafter BS03; Rotunno and Ferretti 2003). Ultimately, only light rainfall occurred over the LMTA and Po Valley during IOP-8 (BS03; Frei and Häller 2001; Medina and Houze 2003; Rotunno and Ferretti 2003). However, asynoptic data presented in BS03 indicate that heavy precipitation and convection did occur during IOP-8, only it was situated over the Ligurian Sea, about 200 km south of where it was forecasted to occur.

Medina and Houze (2003) proposed that the rainfall distribution for IOP-8 was mainly due to the difference in the upstream atmospheric conditions, as determined using the Froude number from the Milan (see Fig. 1) sounding. According to Medina and Houze, during IOP-8, the upstream flow was weak with strong stability. Based on this, Medina and Houze argued that IOP-8 belonged to the blocked flow-around regime. Significant blocking did occur during IOP-8, as discussed in detail by Rotunno and Ferretti (2003). They noted that the cool, moist air impinging on the eastern portion of the Alps was deflected westward into the Po Valley, leading to the development of a cool, stable layer. They further observed that the stable layer appeared to block the warm moist air associated with the low-level jet (LLJ) from reaching the slopes of the Alps resulting in relatively light precipitation over the Po Valley.

The effects of blocking on the nature of convection

Corresponding author address: Dr. Yuh-Lang Lin, Dept. of Marine, Earth, and Atmospheric Sciences, 1125 Jordan Hall, Faucette Drive, NCSU, Raleigh, NC 27695-8208.
E-mail: yl_lin@ncsu.edu

FIG. 1. Alps topography (shaded as in legend) showing sounding locations for Cagliari, Genoa, Milan, and Zadar. The Lago Maggiore target area (LMTA) is also indicated. The star denotes the location of the P-3 dropsounding.

are well established for idealized cases (Chu and Lin 2000; Chen and Lin 2005a,b). The degree of blocking may be measured by the unsaturated moist Froude number upstream of the mountain,

$$F_w = \frac{U}{N_w h}, \tag{1}$$

where U is the uniform incoming flow speed in the direction perpendicular to the mountain ridge, and $N_w = \sqrt{(g/\theta_v)(\partial\theta_v/\partial z)}$ is the unsaturated moist Brunt–Väisälä frequency or buoyancy frequency, and θ_v is the virtual potential temperature. Based on F_w, Chu and Lin (2000) identified three moist flow regimes for conditionally unstable flow over a two-dimensional mountain. They noted that for flows with a low F_w, such as at Milan during IOP-8, the flow is characterized by an upstream propagating convective system, which is induced at the nose of a density current. According to Chu and Lin (2000) both the convection and the stable layer are transient features in the blocked flow regime. Chen and Lin (2005a) extended the study of Chu and Lin (2000) to three-dimensional flow over idealized Alpine mountains and found the critical F_w for an upstream flow with uniform speed and constant N_w is about 0.67.

It seems plausible that the presence of the stable layer in the Po Valley may have altered the location and strength of convection during IOP-8. Indeed, BS03 noted the existence of convergence between the southerly winds associated with the passing trough and the northerly winds of the stable layer. They suggested this convergence may have been responsible for the initiation of convection over the Ligurian Sea. This is consistent with the findings of Reeves and Lin (2004), who noted that the location of maximum convection tended to be collocated with the leading edge of the stable layer in their idealized simulations of IOP-8. Exactly how the stable layer during IOP-8 may have altered the formation of convection has not been well established in the literature.

The nature of the flow into the Po Valley during IOP-8 is consistent with the air motion described in the idealized simulations of Rotunno and Ferretti (2001), who noted that the lower equivalent potential temperature (θ_e) air flowing into the Po Valley from the east "undercuts" the higher θ_e air incident to the Valley from the south. Hence, "as far as the saturated air is concerned, the mountain shape is effectively changed and the vertical motion depends on the slope of the leading edge of the low θ_e blanket." It seems likely that the stable layer in IOP-8 may have acted in the same manner as that described in Rotunno and Ferretti (2001). Such arguments are consistent with the effective mountain arguments of Smith (1985) and Rottman and Smith (1989). Thus, we hypothesize that the strong, stable layer over the Ligurian Sea in IOP-8 behaved as an effective mountain, such that the incident low-level air from the south was lifted up and over the stable layer as though being lifted over terrain. Furthermore, the lifting associated with the effective mountain was sufficient to trigger convection over the Ligurian Sea.

A cursory examination of sounding and reanalysis data suggests the stable layer associated with IOP-8 developed between 0000 and 1200 UTC on 18 October, a full two days before the convection associated with IOP-8 was initiated. This lack of transience in the stable layer for IOP-8 begs the question: What processes are responsible for the stagnation of the stable layer in the Po Valley? Zängl (2003) found in his idealized experiments that the shape of the orography affects the longevity of cold air pools. He noted that for basins completely enclosed by terrain, the stable layer was longer-lived than for cases where the stable layer was positioned on the upstream, unsheltered side of the orography. It is unclear what, if any, effect the sheltering orography (i.e., the Ligurian Apennines) had on the maintenance of the stable layer during IOP-8.

The aim of this research is to (i) assess whether the stable layer during IOP-8 behaved as an effective mountain, (ii) assess the dynamical impacts of the stable layer on the formation of convection during IOP-8, and (iii) examine some factors that may have contributed to the longevity of the stable layer during IOP-8. These goals will be accomplished through analysis of

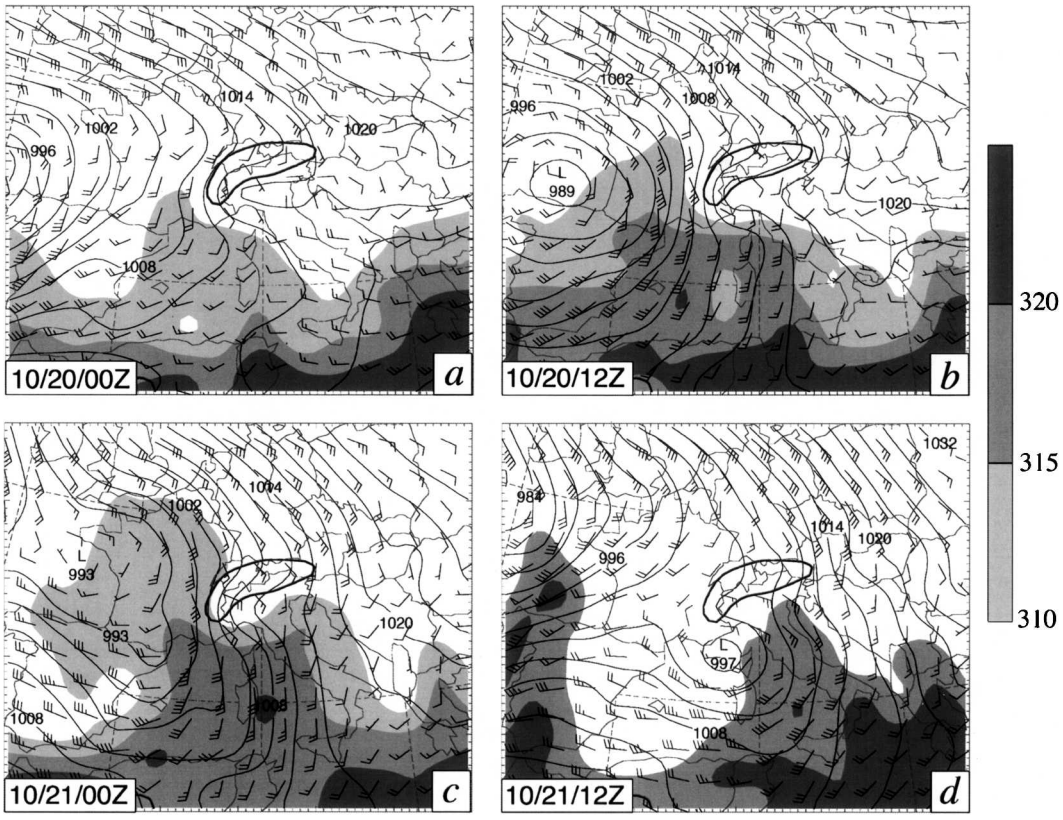

FIG. 2. NCEP 2.5° reanalysis data showing sea level pressure (contoured), 850-hPa equivalent potential temperature (shaded as in legend), and 850-hPa wind barbs (one full barb = 5 m s^{-1}) for (a) 10/20/0000, (b) 10/20/1200, (c) 10/21/0000, and (d) 10/21/1200 UTC, respectively. The 1-km terrain height is denoted by the thick contours.

observed data and numerical simulations. The remainder of this paper is organized as follows. In section 2, an overview of the evolution of synoptic situation for IOP-8 is presented and observed data are compared to model-simulated data in order to test the ability of the model to capture the pertinent flow features. In section 3, the notion of the effective mountain and its impacts on the formation of convection are discussed. Possible mechanisms that contributed to the perseverance of the stable layer are explored in section 4. Finally, conclusions are presented in section 5.

2. Case overview and model verification

a. Evolution of synoptic-scale motion during MAP IOP-8

The primary convective activities for MAP IOP-8 took place between 1200 UTC 20 October (denoted as 10/20/1200) and 1200 UTC 21 October 1999 (10/21/1200). The synoptic-scale evolution of this event has been discussed at length in multiple other papers (BS03; Frei and Häller 2001; Medina and Houze 2003; Rotunno and Ferretti 2003); thus only a cursory overview is provided herein.

According to the National Centers for Environmental Prediction (NCEP) 2.5°-resolution reanalysis data, at 10/20/0000 (Fig. 2a) the low-level large-scale environment was characterized by a surface low pressure center approaching Spain from the west, while a quasi-stationary high pressure region was situated over northern Europe. At 10/20/1200 and 10/21/0000 (Figs. 2b and 2c), a trough separated from the primary low over Spain and extended eastward. By 10/21/1200 (Fig. 2d) a mesoscale low had formed just south of the Maritime Alps. During the time period from 10/20/1200 to 10/21/1200, a strong, southerly low-level jet (with wind speeds between 15 and 20 m s^{-1}) moved eastward and advected air with high θ_e toward the Apennines and Po Valley (Figs. 2b–d). This tongue of high θ_e air did not reach the southern slopes of the Alps, as it was blocked by the preexisting stable layer in the Po Valley.

Figure 3 shows the evolution of the 300-hPa winds and geopotential heights from 10/20/0000 to 10/21/1200. During this period, a ridge can be observed to move

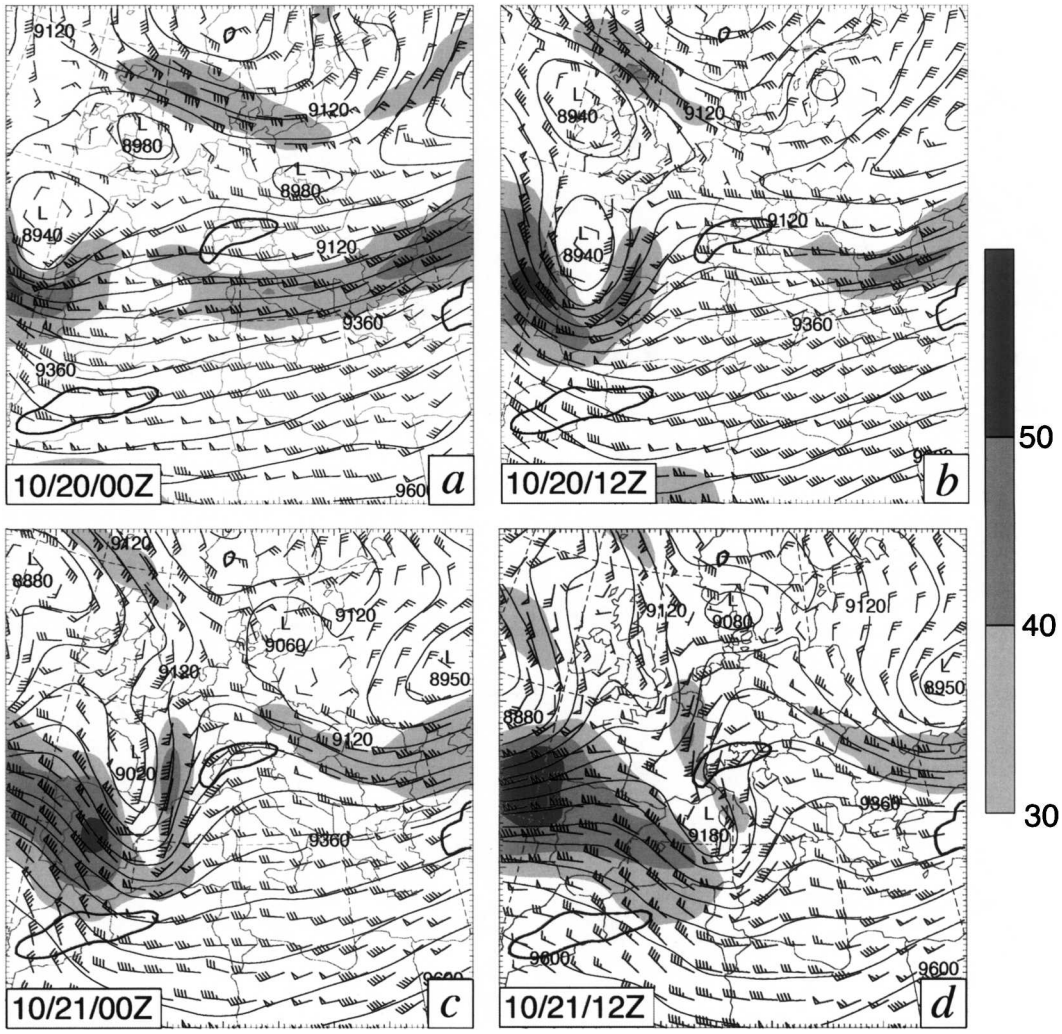

FIG. 3. NCEP 2.5° reanalysis data showing 300-hPa geopotential heights (contoured), 300-hPa wind speeds (shaded as in legend), and 300-hPa wind barbs (one full barb = 5 m s^{-1}) for (a) 10/20/0000, (b) 10/20/1200, (c) 10/21/0000, and (d) 10/21/1200 UTC, respectively. The 1-km terrain height is given by the thick contours.

slowly eastward so that by 10/21/0000 (Fig. 3c), it was directly above Italy. This quasi-stationary ridge appears to have impeded the eastward progression of the trough associated with this same wave leading to a marked shortening of the wavelength of the upper-level wave at the times shown. At 10/21/1200 (Fig. 3d), the entrance region of a jet streak was positioned above the western flank of the Alps and over the Gulf of Genoa, implying the existence of upper-level divergence over the Po Valley, LMTA, and Gulf of Genoa (Van Tuyl and Young 1982). Such a configuration is favorable for heavy orographic precipitation (Buzzi et al. 1998; Lin et al. 2001).

An additional perspective of the large-scale evolution of activities during IOP-8 is provided in Fig. 4, which shows the satellite imagery from 10/20/1800 to 10/21/1200. At each time shown, there is a zone of deep, convective clouds located along the leading edge of the upper-level trough. These convective clouds, which were mainly over southern Europe and the northern Ligurian Sea, propagated eastward with the upper-level trough.

According to Lin et al. (2001), heavy orographic precipitation events are usually accompanied by one or more of nine common ingredients: 1) high precipitation efficiency of the incoming airstream, 2) the presence of a moist, moderate to intense low-level jet, 3) steep orography, 4) favorable (e.g., concave) mountain geometry and a confluent flow field, 5) strong environmentally forced upward motion, 6) the presence of a high moisture flow upstream, 7) a preexisting large convective system, 8) slow (impeded or retarded) movement

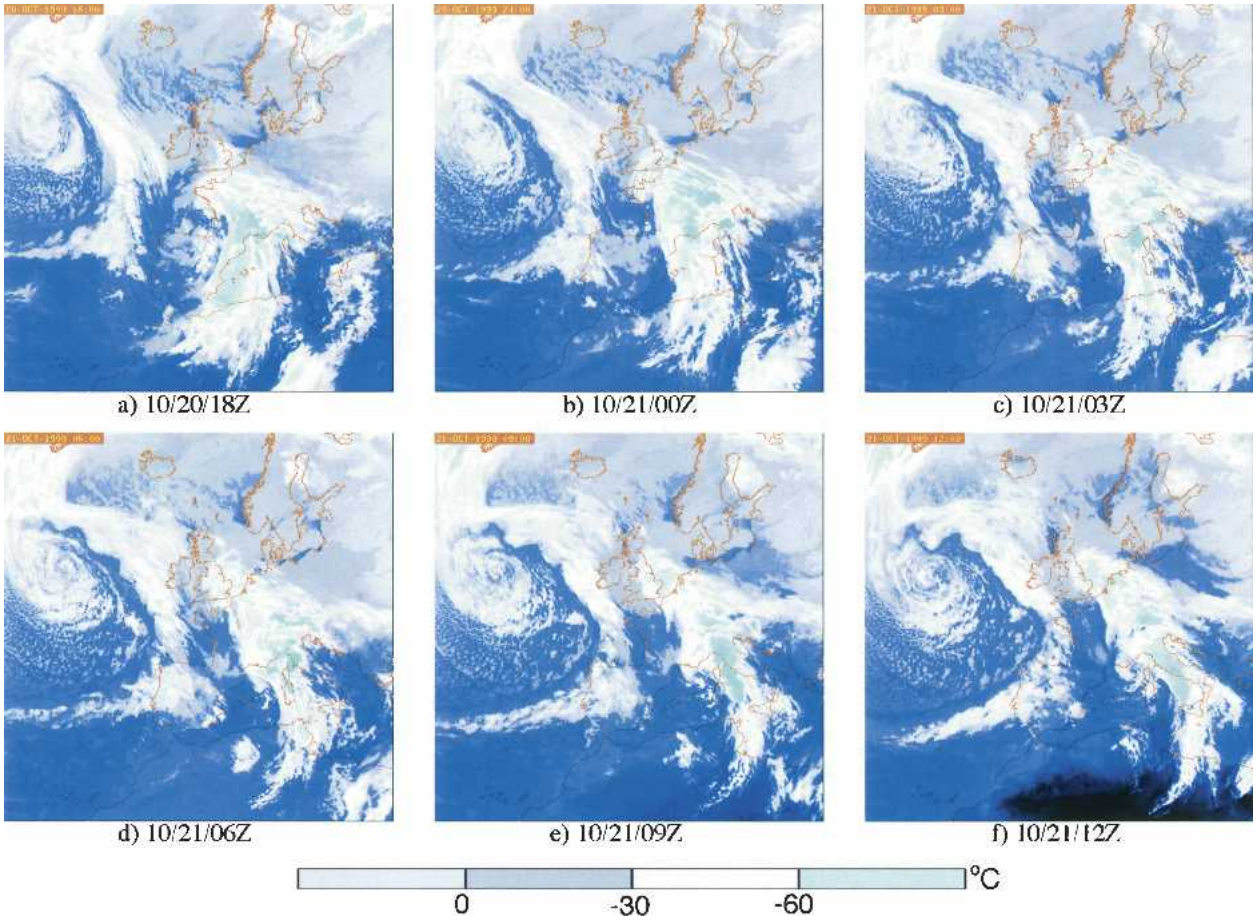

FIG. 4. Meteosat infrared satellite imagery at (a) 10/20/1800, (b) 10/21/0000, (c) 10/21/0300, (d) 10/21/0600, (e) 10/21/0900, and (f) 10/21/1200 UTC, respectively. The shading indicates the blackbody temperatures in °C (see legend in figure).

of the convective system, and 9) high conditional or convective instability of the impinging airstream. The above analyses indicate that many of these ingredients were present during IOP-8. Yet, a rain gauge analysis (Fig. 5) shows the precipitation over the Po Valley and on the upslopes of the Alps was moderate and light during IOP-8. This is echoed in the satellite imagery at 10/21/0300 (Fig. 4c). Note that in the Po Valley and over the southern slopes of the Alps the clouds were comparatively shallow. Conversely, there was a very deep cloud system, indicative of vigorous convection, over the northern Ligurian Sea. Inspection of satellite imagery at later times (Figs. 4d–f) reveals that this cloud system remained well south of the Ligurian Coast.

Additional evidence of the presence of convection over the Ligurian Sea is presented in Fig. 6. This figure shows a cross section composite of radar reflectivity and vertical motion from 10/21/0805 to 10/21/0830 along line AB shown in Fig. 5b. According to this cross section, south of the Apennines ($y \cong -270$ km), there is a convective system with enhanced reflectivity and positive vertical motion. Final evidence of the presence of convection over the Ligurian Sea is provided in Fig. 7, which shows a lightning strike analysis from 10/21/0000 to 10/21/0600 (Fig. 7a) and 10/21/0600 to 10/21/1200 (Fig. 7b). In each of these figures, the heavy lightning strikes appear to be made up of two components: north–south elongated bands over the northern Ligurian and Tyrrhenian Sea and a secondary region of enhanced activity over the Ligurian Sea, just west of Sardinia (apparent only in Fig. 7b). The north–south lines of strikes over the northern Ligurian and Tyrrhenian Seas were produced by the convection associated with the leading edge of the eastward-moving trough. The secondary zone of strikes west of Sardinia may indicate that a convergence zone was present over the Ligurian Sea along which convection was generated and/or enhanced, consistent with the findings of BS03.

Soundings at 10/21/0000 from Cagliari, Genoa, and Milan, as well as the dropsounding from the P-3 flight mission taken at 10/21/0800 (see Fig. 1 for sounding

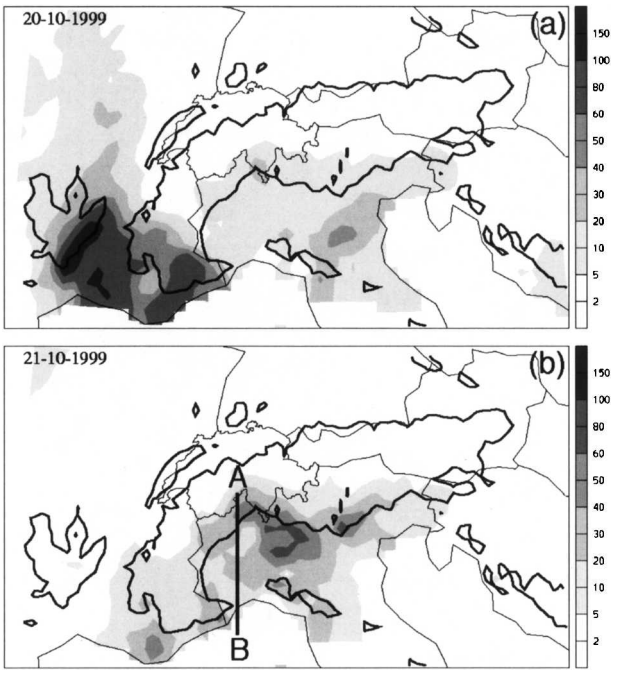

FIG. 5. Accumulated precipitation (mm) (a) from 10/20/0600 to 10/21/0600 and (b) from 10/21/0600 to 10/22/0600.

locations), are shown in Fig. 8. The most important feature of note in the Milan, Genoa, and P-3 soundings is the very well defined stable layer near the surface as was noted in Medina and Houze (2003), Rotunno and Ferretti (2003), and BS03. The dropsounding (Fig. 8c) shows that the cool, stable layer protruded well into the northern Ligurian Sea. The stable layer in these three soundings was characterized by easterly winds. Above the stable layer, the winds were from the south. The Cagliari sounding (Fig. 8d) is comparatively warmer and less stable than the P-3, Genoa, and Milan soundings. The inversion in the Cagliari sounding at about 1000 m was associated with the northward advection of hot, dry air off of the Atlas Mountains, leading to the development of an elevated mixed layer (Tripoli et al. 2000). The winds throughout the lower troposphere in the Cagliari sounding were from the south. As discussed in BS03, comparison of the low-level winds upstream of the stable layer with those within the stable layer imply there was a convergence zone over the Ligurian Sea that may have aided in the development of convection over the Ligurian Sea. Further scrutiny of the Milan, Genoa, and P-3 soundings shows there was a warm, less stable layer with southerly/southwesterly winds residing atop the cool, stable layer near the surface. This stratification of temperature and wind direction is similar to that often observed in a warm front and implies that the air from the south may have overridden the stable layer. Above the inversion, the wind direction is southerly and the stability and moisture characteristics are similar to those upstream of the stable layer.

Our ability to fulfill the objectives of this research is limited by a lack of surface-based observations over the Ligurian Sea, such as radar and rain gauge measurements. We are further limited by the spatial and temporal resolution of the available analysis data. A numerical simulation of the event can provide a surrogate dataset with greater temporal and spatial resolution, allowing for a more meaningful analysis of the major goals of this research. Numerical simulation of the event also allows for sensitivity tests to assess the factors responsible for the maintenance of the stable layer.

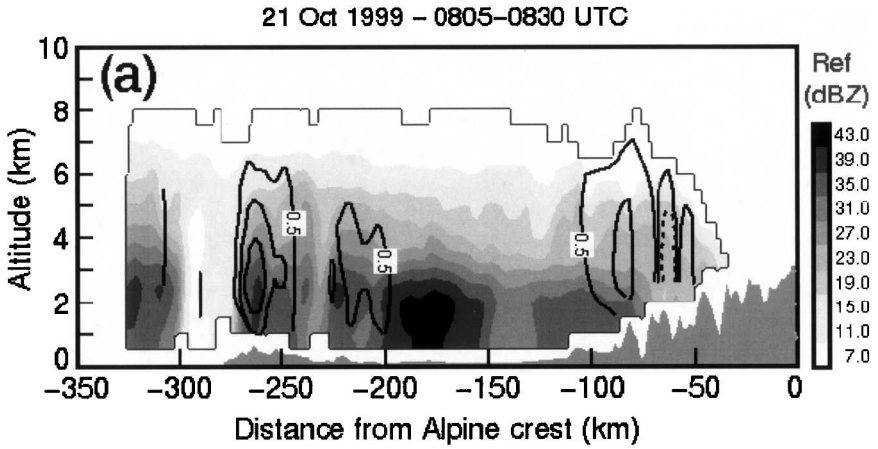

FIG. 6. Meridional cross section along line AB in Fig. 5b showing radar reflectivity (see legend on right-hand side) and positive vertical velocity in steps of 0.5 m s^{-1} starting at 0.5 m s^{-1}. Dashed contours indicate regions where vertical velocity is less than 0 m s^{-1}. (Adopted from Fig. 8a of Bousquet and Smull 2003.)

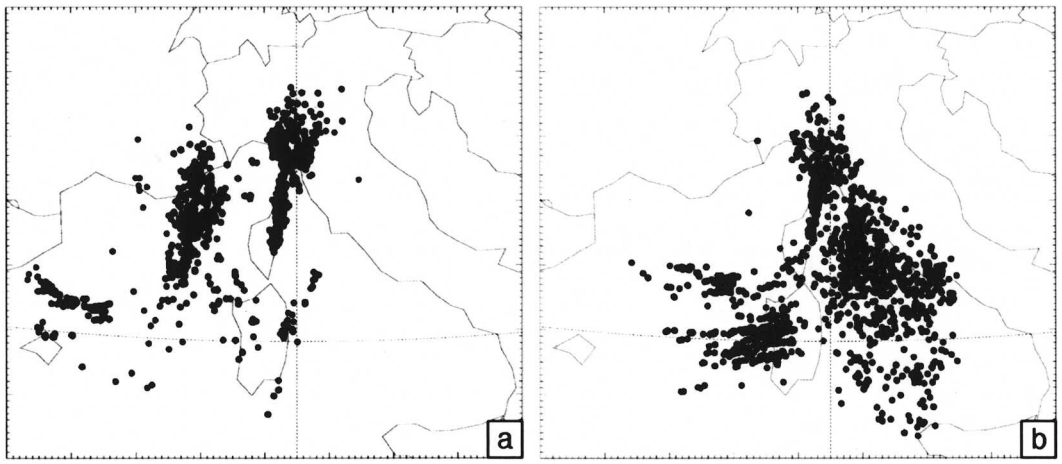

FIG. 7. Lightning strikes from (a) 10/21/0000 to 10/21/0600 and (b) 10/21/0600 to 10/21/1200.

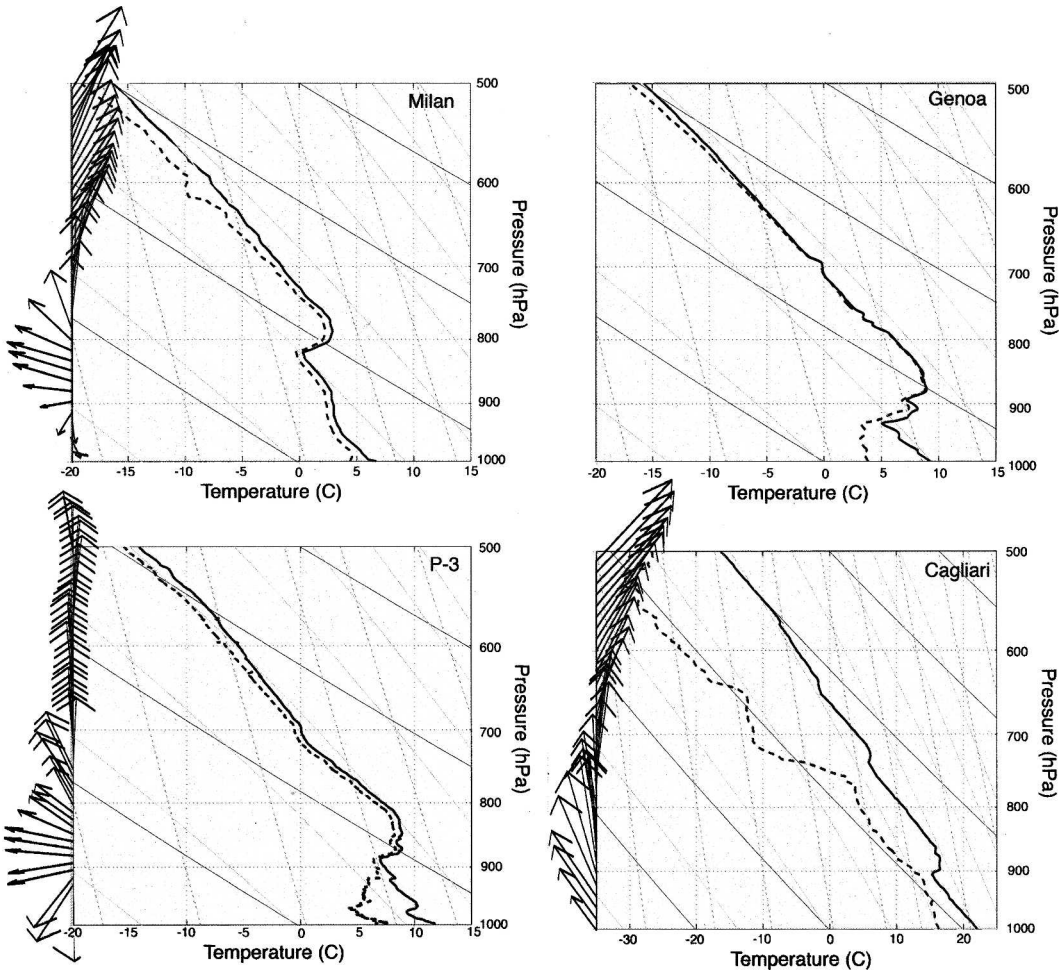

FIG. 8. Observed soundings from (a) Milan, (b) Genoa, and (d) Cagliari at 10/21/0000, and (c) the P-3 dropsounding at 10/21/0800. Temperature is given by the solid contours, and dewpoint temperature is given by the dashed contours. Wind speed and direction are given on the left-hand side of each panel. (No wind information was available for the Genoa sounding.)

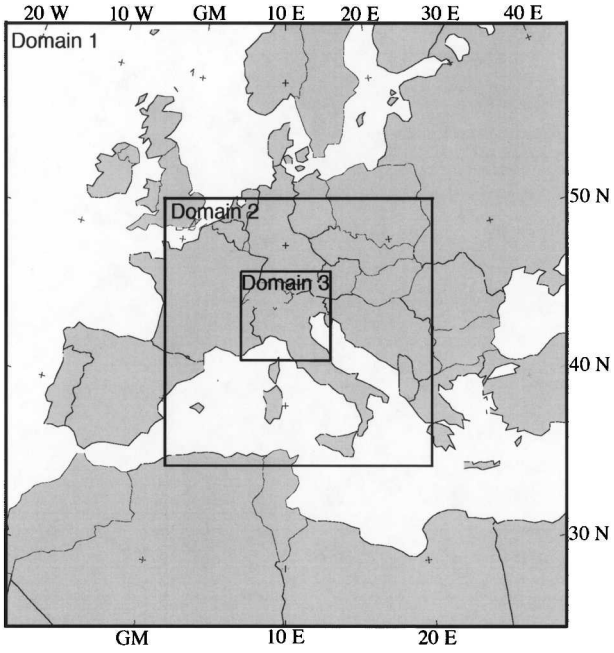

FIG. 9. Computational domains used in MM5 simulations.

b. Model description and experimental design

The fifth-generation Pennsylvania State University–National Center for Atmospheric Research (PSU–NCAR) Mesoscale Model (MM5, version 3.5) (Dudhia 1993) was used to simulate MAP IOP-8. The model solves the fully compressible, nonhydrostatic governing equations in $\sigma - p$ coordinates. Three nested computational domains were used in all simulations with the outer, middle, and inner domains having grid spacings of 45, 15, and 5 km, respectively. These domains are shown in Fig. 9. All domains used the Goddard Lin–Farley–Orville microphysical parameterization scheme (Lin et al. 1983; Tao and Simpson 1993), Blackadar (1979) planetary boundary layer parameterization, 45 σ levels, and a terrain resolution of 5 km. The cumulus parameterization schemes used are the Betts–Miller (1993) scheme for the outer domain and the Grell (1993) cumulus scheme for the inner domains. The simulation was initialized at 10/19/1200 using the NCEP reanalysis data and integrated for 60 h. The inner domains (domains 2 and 3) were started 6 h after the parent domain (domain 1). Output from domain 2 (15-km grid spacing) will be used in all subsequent figures and discussions unless otherwise noted. We have chosen to focus on the output from domain 2 because it has the necessary resolution and horizontal extent to resolve the features of interest.

c. Model verification

The CNTL simulation compares well to the NCEP reanalyses. Figure 10a, which may be compared to Fig. 3d, shows 300-hPa heights, wind speeds, and wind barbs from the 45-km resolution (domain 1) simulation at 10/21/1200. As shown in the NCEP reanalyses, there was a jet streak positioned over the concave region of the Alpine ridge extending northwestward, over the

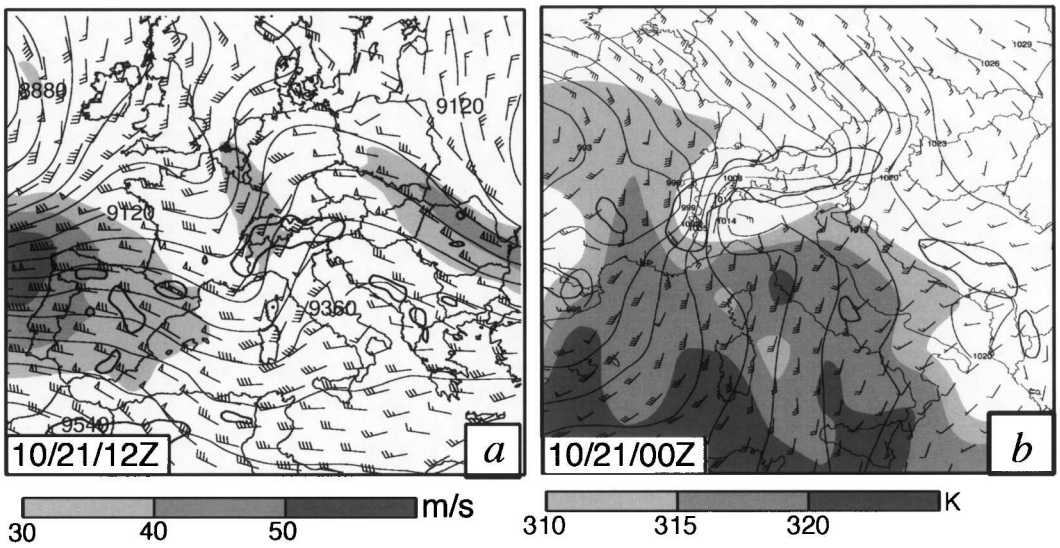

FIG. 10. MM5 45-km-resolution simulation output showing (a) 300-hPa geopotential (contoured), 300-hPa wind speeds (shaded as in legend), and 300-hPa wind barbs (one full barb = 5 m s^{-1}) at 10/21/1200 and (b) sea level pressure (contoured), 850-hPa equivalent potential temperature (shaded as in legend), and 850-hPa wind barbs (one full barb = 5 m s^{-1}) at 10/21/0000.

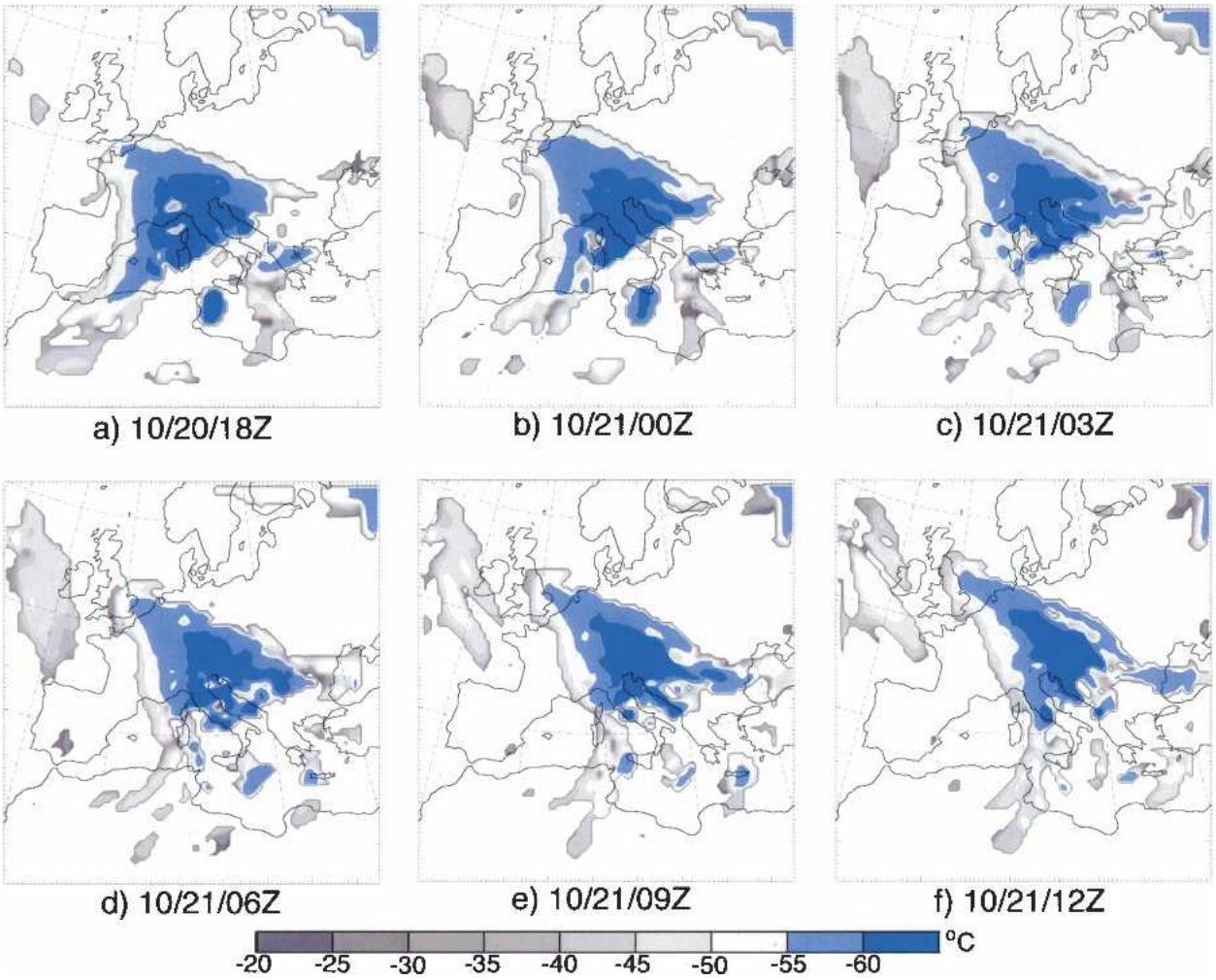

FIG. 11. MM5 45-km-resolution simulated cloud-top temperatures (shaded as in legend) at (a) 10/20/1800, (b) 10/21/0000, (c) 10/21/0300, (d) 10/21/0600, (e) 10/21/0900, and (f) 10/21/1200 UTC, respectively.

border between France and Germany. This jet streak was positioned such that its entrance region was situated over the southern Alpine region (Fig. 10a). Throughout the integration period, the upper-level wave deepened and the wavelength shortened, as was noted in the reanalysis data (Fig. 3).

Figure 10b shows the sea level pressure and 850-hPa wind and θ_e fields at 10/21/0000. According to this figure, the low-level features compare well with the reanalysis data (Fig. 2c). In Fig. 10b, θ_e values were significantly lower in the LMTA than those in the moist tongue (294 versus 324 K), and the flow was from the east rather than from the south, indicating the presence of a cool, dry air mass in the LMTA. A southerly low-level jet advecting high θ_e air impinged on the stable layer in the Po Valley with maximum θ_e regions located near the coast and in the northern Italian peninsula. As in the observations (Fig. 2), the high θ_e air did not penetrate into the LMTA at this level during the CNTL simulation.

The ability of the model to capture the general pattern and propagation of convective systems was determined through comparison of simulated cloud-top temperatures (Fig. 11) with the satellite-measured cloud-top temperatures (Fig. 4). Comparison of Fig. 11 with Fig. 4 shows that the pattern and intensity of the convective area was well captured in the simulation. The area of strong convection with cloud-top temperatures less than -60°C simulated by the model at 10/20/1800 was located over the Ligurian Sea and Po Valley (Fig. 11a), roughly consistent with the satellite imagery (Fig. 4a). The simulated area of strong convection then moved toward the northeast over the next 12 h (Figs. 11b–d), showing good agreement with the observations (Figs. 4b–d). Between 10/21/0600 and 10/21/1200 (Figs. 11d–f) the simulated area of convection propagated

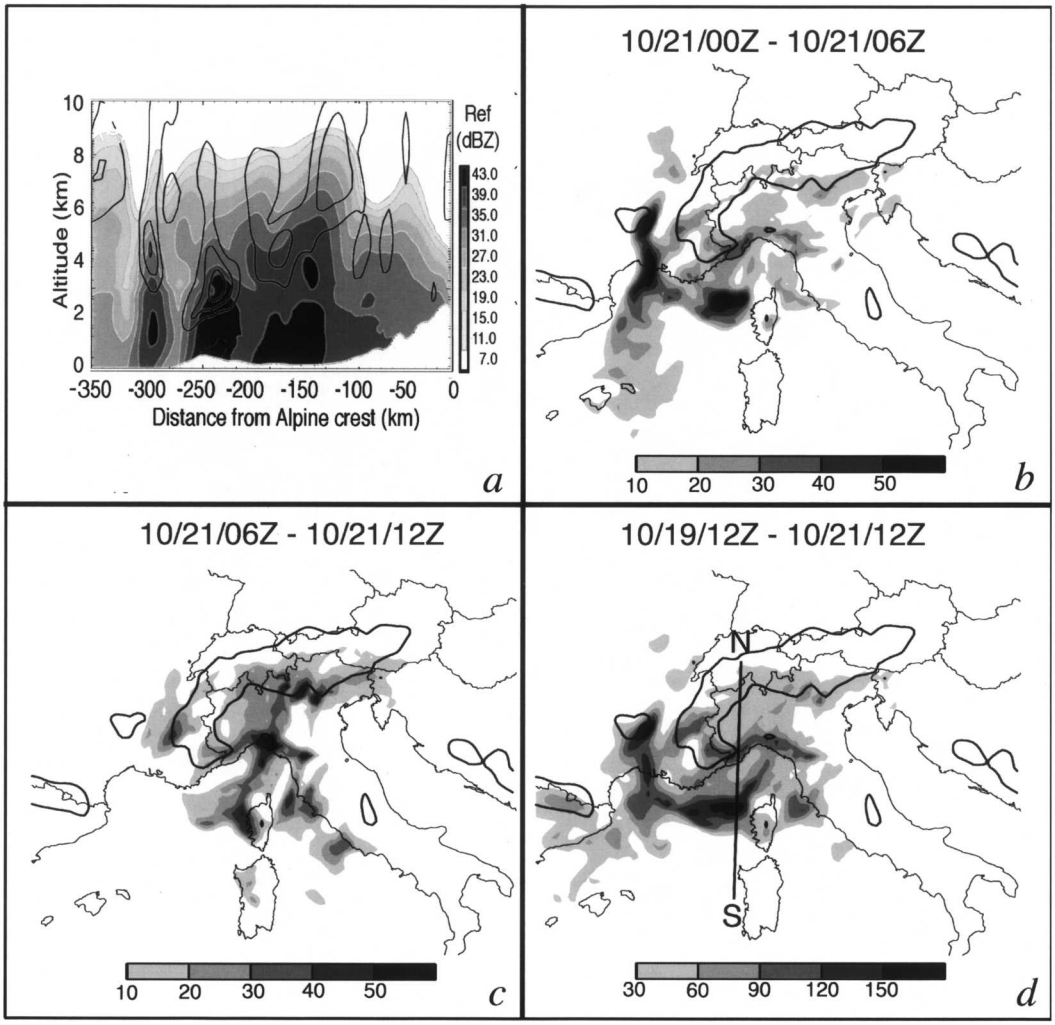

FIG. 12. MM5 15-km-resolution simulation output showing (a) model-derived reflectivity (shaded as in legend on right-hand side) and positive vertical motion contoured every 0.3 m s^{-1} starting at 0.3 m s^{-1} along the cross section shown in Fig. 5b, and accumulated precipitation from (b) 10/21/0000 to 10/21/0600, (c) 10/21/0600 to 10/21/1200, and (d) 10/19/1200 to 10/21/1200 UTC, respectively.

eastward at a faster pace than in the observations (Figs. 4d–f). For example, the satellite imagery at 10/21/0900 (Fig. 4e) shows that the area of cloud-top temperatures less than −60°C was mainly over Italy and upstream of the Apennines. In contrast, the simulated area of strong convection for the same time was located over northeast Italy (Fig. 11e).

Further evidence that the model adequately captured the convective activities is provided in Fig. 12a, which shows the model-simulated radar reflectivity at 10/21/0800 along the cross section shown in Fig. 5b. As in the observed radar reflectivity (Fig. 6), the simulated reflectivity (Fig. 12a) shows the existence of deep, convective cores off the Ligurian Coast. Six-hourly accumulated precipitation (Figs. 12b and 12c) shows that as the upper-level trough moved eastward, heavy precipitation fell just west of Corsica (Fig. 12b). As the trough moved past Corsica, after 10/21/0600, moderate precipitation amounts accumulated on the upslopes of the Ligurian Apennines (Fig. 12c). Comparison of Figs. 12b and 12c to Figs. 7a and 7b, respectively, shows good agreement between the locations of maximum precipitation and maximum strike locations. This agreement implies the timing and intensity model-simulated precipitation is reliably close to the actual event. The 48-h accumulated precipitation from 10/19/1200 to 10/21/1200 (Fig. 12d) shows that the precipitation over the Po Valley and LMTA was even and light, which agrees well with the rain gauge analyses presented in Fig. 5.

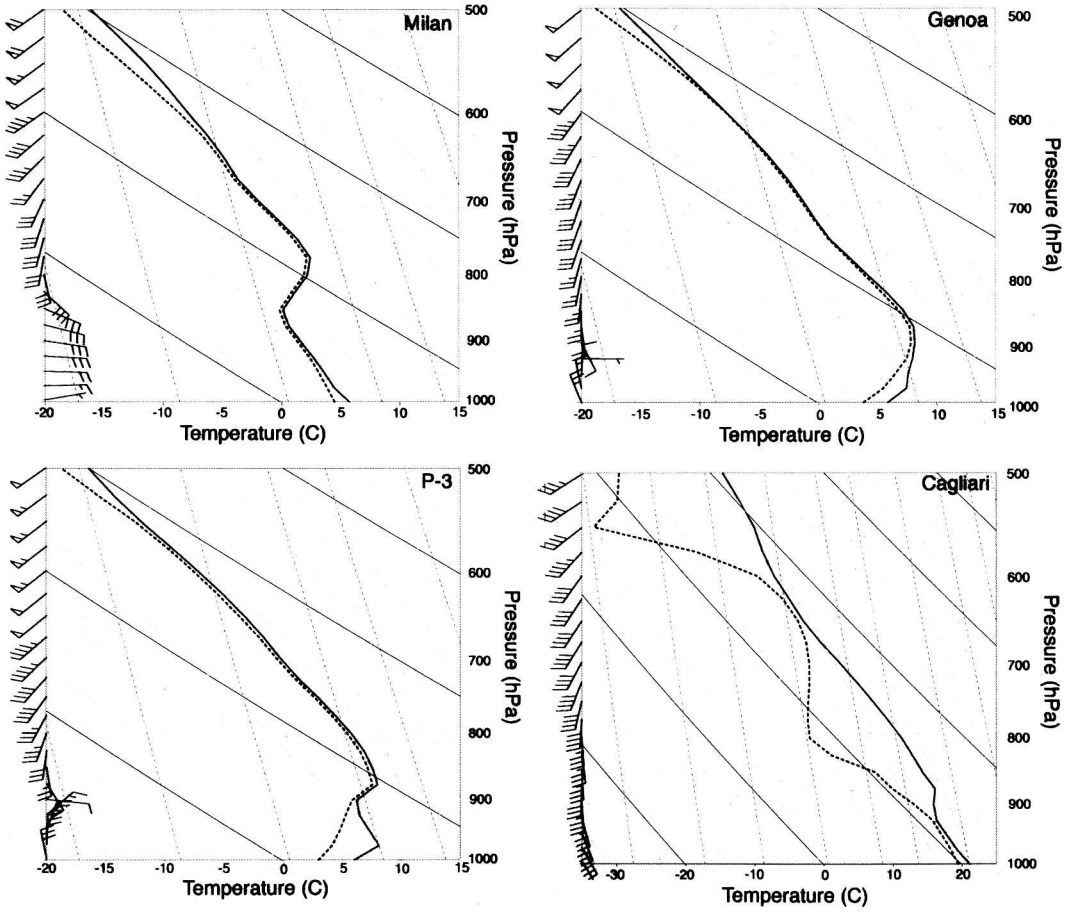

FIG. 13. MM5 15-km-resolution simulation output showing soundings at (a) Milan, (b) Genoa, and (d) Cagliari at 10/21/0000, and (c) the P-3 dropsounding location at 10/21/0800. Wind barbs for each sounding are given on the left-hand side of each panel (one full barb = 5 m s^{-1}). Temperature is given by the solid contours, and dewpoint temperature is given by the dashed contours. Wind speed and direction are given on the left-hand side of each panel.

Further evidence of the model's ability to adequately capture the important flow features associated with this event is provided in Fig. 13, which shows model-simulated soundings at 10/21/0000 from Milan, Genoa, Cagliari, and the P-3 dropsounding location. The model output soundings at Milan, Genoa, and the P-3 location compare well with the observed soundings (Fig. 8) and show the presence of a stable layer at the surface with easterly winds capped by a less stable, near-saturated layer with southerly winds. The simulated Cagliari sounding (Fig. 13d) also has good agreement with the observed Cagliari sounding (Fig. 8d), showing a near-neutral layer of air near the surface over which an elevated mixed layer resides and southerly winds throughout the lower troposphere. The good agreement between the observations and model output implies the model adequately captured the observed synoptic, thermodynamic, and convective characteristics of IOP-8 and, therefore, is adequate for use to further address the main questions of this research.

3. Dynamical impacts of the stable layer

a. Effective mountain

Rotunno and Ferretti (2003) argued that when there is significant blocking of low θ_e air along the eastern portion of the Alps, the cool, stable air is deflected westward, into the Po Valley. This low-lying, stable air mass may then behave as an impediment to airstreams incident to the Po Valley from the south. In other words, the stable air mass may behave, effectively, as a mountain to the incoming southerly winds. Rottman and Smith (1989) have also noted this behavior in their tank experiments of low Froude number flow over an obstacle; they refer to these layers as *effective mountains*. There is evidence in previously published work

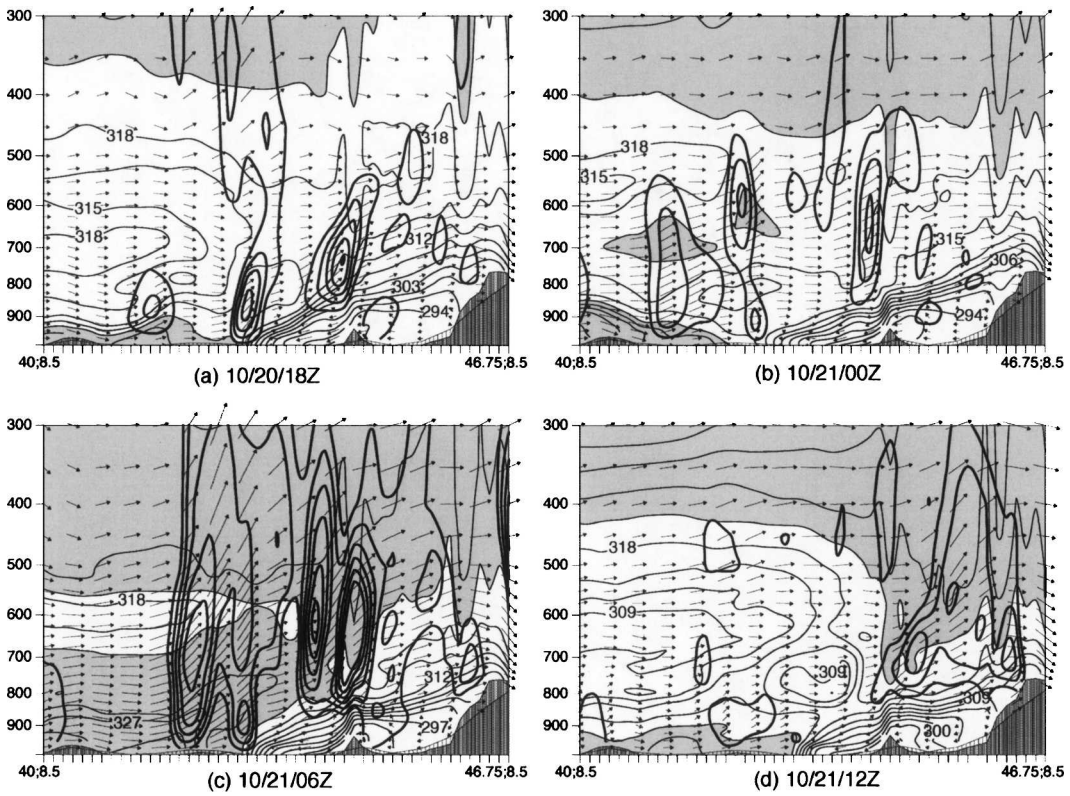

FIG. 14. MM5 15-km-resolution simulation output showing vertical cross section of θ_e (thin, solid contours; values > 321 K are shaded), wind vectors, and positive vertical motion (thick contours, contoured every 10 Pa s^{-1} starting at -10 Pa s^{-1}) along line NS in Fig. 12d for (a) 10/20/1800, (b) 10/21/0000, (c) 10/21/0600, and (d) 10/21/1200.

that suggests the stable layer during IOP-8 may have behaved as an effective mountain. For example, the trajectory analysis in Rotunno and Ferretti (2003, their Fig. 8f) shows a rapid ascent from 0.75 to 1.5 km over a 1-h period over the Ligurian Sea. Once over the Po Valley, the ascent along this trajectory was significantly less.

Figure 14 shows a north–south cross section (depicted as line NS in Fig. 12d) of θ_e, wind vectors and upward motion ($-\omega$) fields from 10/20/1800 to 10/21/1200. Notice that the stable layer was present at 10/20/1800 and 10/21/0000 (Figs. 14a and 14b), extending southward from the Alps over the Ligurian Sea so that at all times shown, its leading edge was positioned about 100 km upstream of the Apennines. Although the temperature gradient across the stable layer appears to be slightly stronger during the convection (Fig. 14c), it was not significantly impacted by the convection. This is different from the blocking presented in Chu and Lin (2000), where the stable layer and convection appear to have acted in a mutually enhancing manner as they propagated upstream in conjunction with one another.

In Figs. 14a–c, which show times before the trough had passed, there are two convective systems located along the slope of the cold dome: one at the leading edge of the cold dome and the other slightly south of and above the Ligurian Apennines. We hypothesize that lifting by the leading edge of the effective mountain is responsible for the plume of positive vertical motion along the leading edge of the effective mountain, as will be discussed in the following two subsections. The more elevated convective system farther downstream is likely enhanced by two factors. Careful inspection of the slope of the θ_e contours shows that just upstream of the Apennines, the θ_e contours become more vertically aligned. Assuming $w \propto U\partial\theta_e/\partial y$, which is equivalent to $w \propto U\partial h/\partial y$ for flow over real mountains, where h is the height of the mountain, then this location where the contours become more vertical should be accompanied by enhanced vertical motion, as evidenced in Figs. 14b and 14c. This same argument holds true for the leading edge of the cold dome, where the θ_e contours also adopt a more vertical orientation. We also note that for airstreams incident to the cold dome, the level of free convection is located at 775 hPa. The top of the cold dome intersects this level just upstream of the Apennines, at the same location as the zone of

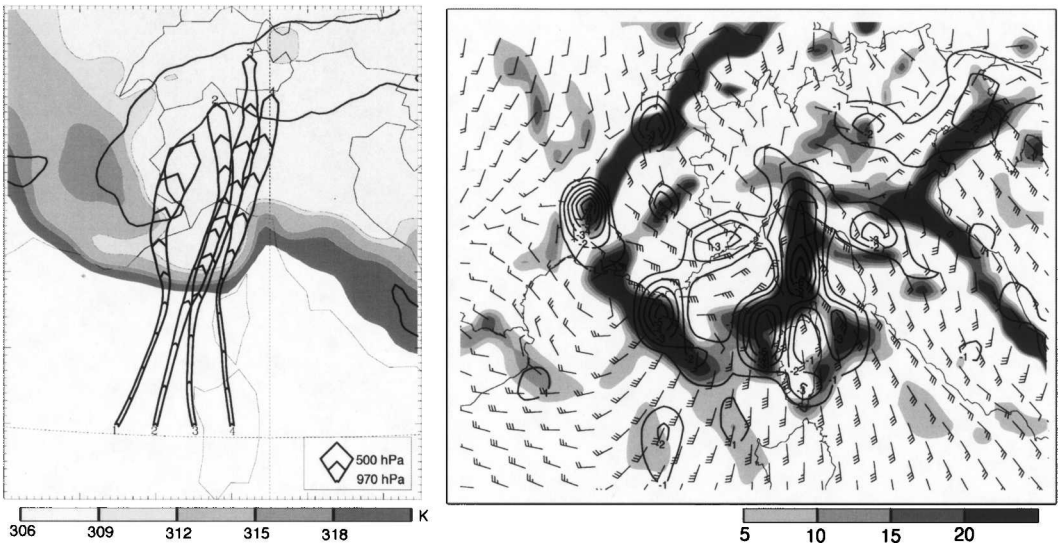

FIG. 15. MM5 15-km-resolution simulation output showing (a) forward trajectory analysis for parcels originating at $\sigma = 0.95$ starting at 10/21/0300 and ending at 10/21/1200 and surface θ_e at 10/21/0600 (shaded as in legend). The width of the ribbon denotes the height of the parcel (see legend in lower right of panel). (b) Surface convergence ($\times 10^{-5}$ s^{-1}; shaded as in legend), surface wind barbs, and 850-hPa upward vertical motion (Pa s^{-1}; contoured) at 10/21/0600.

positive vertical motion. Hence, vertical ascent was enhanced because the parcels became buoyantly unstable. Returning to the precipitation analyses shown in Figs. 12b and 12c, we can see that each of the zones of positive vertical velocity are accompanied by a maximum in precipitation: one over the Ligurian Sea, just west of Corsica, and the other along the Ligurian Coast.

The simulated wind vectors (Fig. 14) show that the southerly airstream impinging on the stable layer was lifted *over* the stable layer and rose parallel to the slope of the stable layer, thus experiencing only gradual lifting above the Po Valley. Further inspection of Fig. 14 shows that as time progressed, the temperature and moisture characteristics on either side of the cold dome remained fairly constant. It appears as though the cold dome in the CNTL simulation behaved as a material surface, or an effective mountain, causing the less dense air associated with the LLJ to be gently lifted over the Po Valley rather than sinking in the lee of the Ligurian Apennines and then experiencing an abrupt lifting by the Alps.

In addition to the vertical ascent at low levels along the leading (southern) edge of the cold dome, which appeared in the period between 10/20/1800 and 10/21/0600 (Figs. 14a–c), the wind vectors indicate there was a broad, deep region of weak ascent found both upstream of and over the cold dome. This broader, less localized zone of ascending air appears to be due to baroclinic forcing. However, further sensitivity studies wherein the stable layer is removed would need to be performed to verify this notion. Such an experiment is beyond the scope of this work and will be addressed in a separate study.

Additional evidence that the stable layer may have behaved as an effective mountain is provided in the trajectory analysis shown in Fig. 15a. This figure shows a forward trajectory analysis of parcels initially at a height of $\sigma = 0.95$ and upstream of the effective mountain, as indicated by large gradient in θ_e. Notice that as the parcels encountered the stable layer, they experienced an abrupt lifting similar to that shown in Rotunno and Ferretti (2003). In addition, the leading edge of the effective mountain forms an arc shape that roughly extends from Nice, France, to Pisa, Italy. Figure 15b shows the numerically simulated surface winds and convergence along with upward motion at 850 hPa at 10/21/0600. In this figure, the surface convergence and low-level vertical ascent form an arc shape that is consistent in position with the leading edge of the effective mountain.

If the stable layer did act as an effective mountain, extending from the Alps to the Ligurian Sea, then the removal of the Ligurian Apennines, which are beneath the effective mountain surface, should have insignificant effects on triggering the convective systems over the Ligurian Sea. To test this idea, a simulation (NOAP) was performed in which a portion of the Apennines along the northern Ligurian Coast was removed. The modified terrain in this simulation is shown

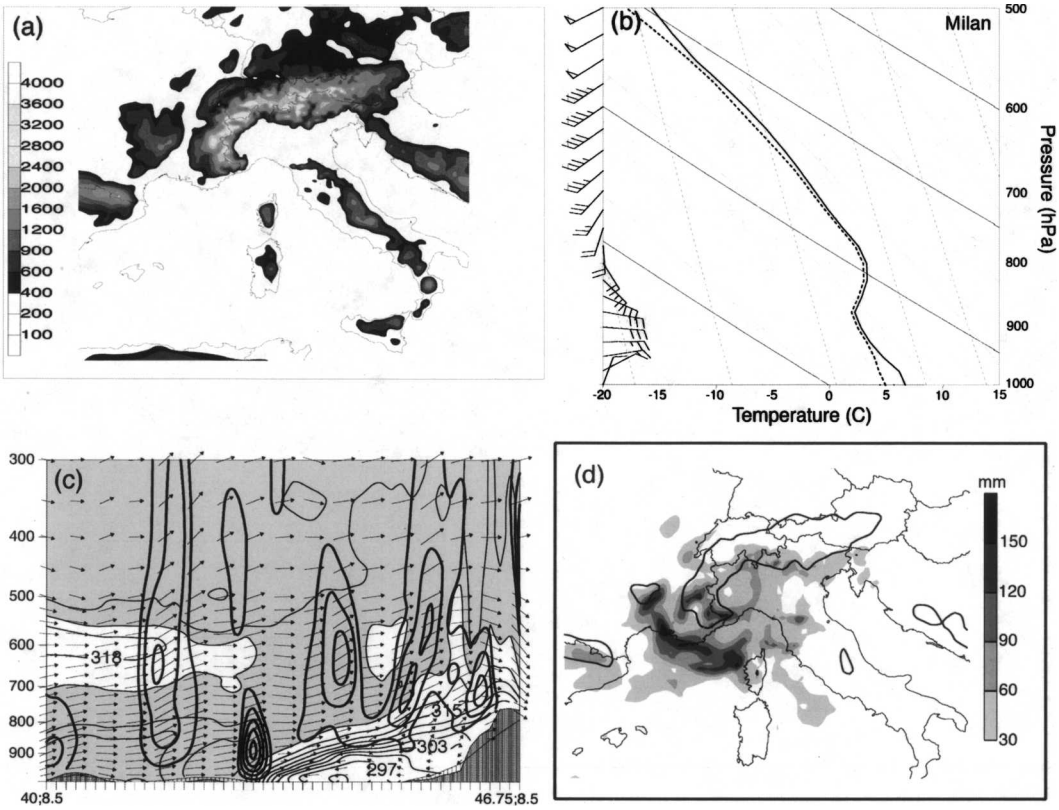

FIG. 16. NOAP 15-km-resolution simulation output showing (a) terrain, (b) Milan sounding at 10/21/0000 (as in Fig. 11a), (c) vertical cross section at 10/21/0600 as in Fig. 14c, and (d) accumulated precipitation from 10/19/1200 to 10/21/1200.

in Fig. 16a. Figure 16b shows the NOAP simulated sounding from Milan. Comparison of Fig. 16b to Fig. 13a, which shows the corresponding sounding from the CNTL simulation, reveals that the temperature inversion at the top of the stable layer was marginally weaker in the NOAP simulation and that the depth of the stable layer was slightly lower than that in the CNTL simulation. However, the basic thermal structures of the atmosphere in the vicinity of Milan are very similar for the NOAP and CNTL soundings.

An additional perspective of the flow in the absence of the Apennines is provided in Fig. 16c, which shows a cross section from the NOAP simulation at 10/21/0600. Comparison of Fig. 16c and the corresponding cross section from the CNTL simulation (Fig. 14c) shows generally good agreement. However, some differences do exist. Among these is that the temperature gradient along the leading edge of the stable layer appears to be greater in the NOAP simulation than that in the CNTL simulation. It appears that the Apennines acted to partially block the stable layer from exiting the Po Valley to the south. This finding is consistent with Zängl (2003), who found that when orography exists on the upstream side of a cold pool, the rate of cold pool erosion was significantly reduced. Comparison of the depth of the cold dome in Figs. 16b and 16c with Figs. 13a and 14c, respectively, shows that in the Po Valley, the cold dome was deeper in the CNTL simulation than in the NOAP simulation.

In Fig. 16c, the leading edge of the stable layer is still characterized by a zone of positive vertical velocity, as in the CNTL simulation (Fig. 14c). However, there is no steepening of the slope over the Ligurian Coast in the θ_e field for the NOAP simulation, and the top of the cold dome does not intersect with the level of free convection until well over the Po Valley in the NOAP simulation. These differences in the slope of the cold dome did impact the precipitation field, as can be assessed through comparison of Figs. 12d and 16d. As found in the CNTL simulation (Fig. 12d), there is a line of precipitation maxima over the Ligurian Sea that extends from Nice to Corsica. However, the precipitation maxima that was present along the Ligurian Coast in the CNTL simulation is not present in the NOAP simulation (Fig. 16d). Rather, there were increased precipitation accumulations on the upslopes on the Alps.

b. Upstream flow conditions

Medina and Houze (2003) used the Froude number, defined as $F_r = U/Nh$, diagnosed from the Milan sounding to determine the flow regime and thus explain the lack of convection over the Po Valley and LMTA in IOP-8. Herein, we attempt a similar diagnosis for the effective mountain in order to better understand why convection was incited at the leading edge of the effective mountain. There are two soundings that can be used for this purpose: one at Ajaccio, Corsica (which is shown in BS0; Fig. 9b), and the other at Cagliari. The Ajaccio sounding is on the lee side of a mountain and is considerably drier and more stable than the Cagliari sounding. Comparison of these soundings with other model-derived soundings upstream of the effective mountain shows that the Cagliari sounding is a better representative of the upstream flow conditions. This is consistent with the findings of Asencio et al. (2003). The Cagliari sounding (Fig. 13d) has a relatively low lifting condensation level (LCL) of 926 hPa, which is lower than the height of the effective mountain meaning that lifting by the effective mountain was sufficient to induce condensation. This sounding was also conditionally unstable. It had a CAPE of 1443 J kg^{-1}. However, the level of free convection (LFC) was rather high (775 hPa), implying that lifting by the leading edge of the effective mountain alone was not sufficient to release conditional instability and trigger convection. Yet, the lifting above the effective mountain appears to have been enhanced by upper-level divergence (Fig. 10a). These combined forcings for lifting may be responsible for the development of deep convection and heavy rainfall.

If we use the height of the leading edge of the effective mountain (h = 1 km) and the temperature and winds from the 1000–850-hPa layer in the calculation of F_w, a value of 1.2 is obtained. This value is very large compared to the critical F_w (0.67) proposed by Chen and Lin (2005a), which indicates the flow over the leading edge of the effective mountain belonged in regime III of Chen and Lin. This flow regime is characterized by a stationary precipitation system and significant accumulated precipitation along the peak or upslope of the terrain (i.e., over the Ligurian Sea in the present case). An estimation of F_w using the height of the Alps (2 km) for this sounding gives a value of 0.60; this value is considerably larger than that calculated using the Milan sounding (0.12). Although 0.60 is slightly less than the critical moist Froude number, it is sufficiently close to a value that one might expect that with many of the common ingredients present (Lin et al. 2001; also briefly discussed in section 2a); thus, heavy precipitation could have occurred over the LMTA. Very similar moist Froude number values were obtained using the observed sounding from Cagliari at 10/21/0000.

c. Triggering of convection

It is well documented that orographic lifting is often a primary cause of heavy orographic precipitation and that steeper terrain is associated with heavier precipitation (e.g., Smith 1979; Neiman et al. 2002; Buzzi et al. 1998; Rotunno and Ferretti 2001; Gheusi and Stein 2003; Stein 2004). Lin et al. (2001) argued that vertical motion (w) can be decomposed into two different elements:

$$w = w_{\text{oro}} + w_{\text{env}}, \tag{2}$$

where w_{oro} is the orographically forced upward motion, and w_{env} is the upward motion induced by other processes in the environment, such as synoptically induced circulations and/or instabilities. Lin et al. (2001) further argued that w_{oro} can be approximated by the basic wind and the slope of the topography:

$$w_{\text{oro}} = \frac{Dh}{Dt} = \mathbf{V}_h \cdot \nabla h, \tag{3}$$

where $h(x, y)$ is the terrain height, and $\mathbf{V}_h$ is the horizontal wind vector. This implies that the positive *orographic moisture flux*, which is proportional to upslope precipitation (Alpert 1986; Doswell et al. 1998), can be written as

$$w_{\text{oro}}q = (\mathbf{V}_h \cdot \nabla h)q, \tag{4}$$

where q is the mixing ratio. In Eq. (4), if $\nabla h < 0$, $w_{\text{oro}}q$ is assumed to be zero. To assess the contribution to the moisture flux by orographic lifting, $w_{\text{oro}}q$ was evaluated at σ = 0.995. Figure 17a shows the results of this calculation based on the 15-km-resolution simulated results. Maxima of $w_{\text{oro}}q$ are located along the upslopes (i.e., southern slopes) of the Alps, Apennines, Corsica, and Sardinia mountains. The maximum $w_{\text{oro}}q$ along the Ligurian Coast coincides with the maximum of precipitation shown in Fig. 12c.

In addition to the orographic lifting by the real terrain, the upward motion produced by the environment (w_{env}) may also contribute to the precipitation. The total vertical moisture flux, wq, evaluated at σ = 0.995 is plotted in Fig. 17b. Notice there exist two regions of positive wq away from the terrain, over the Ligurian Sea. This indicates some other source of lifting, other than by the real terrain, was present over the Ligurian Sea. The lack of positive wq over the upslopes of the Alps may suggest moisture was depleted from the incoming airstream by the convection over the Ligurian

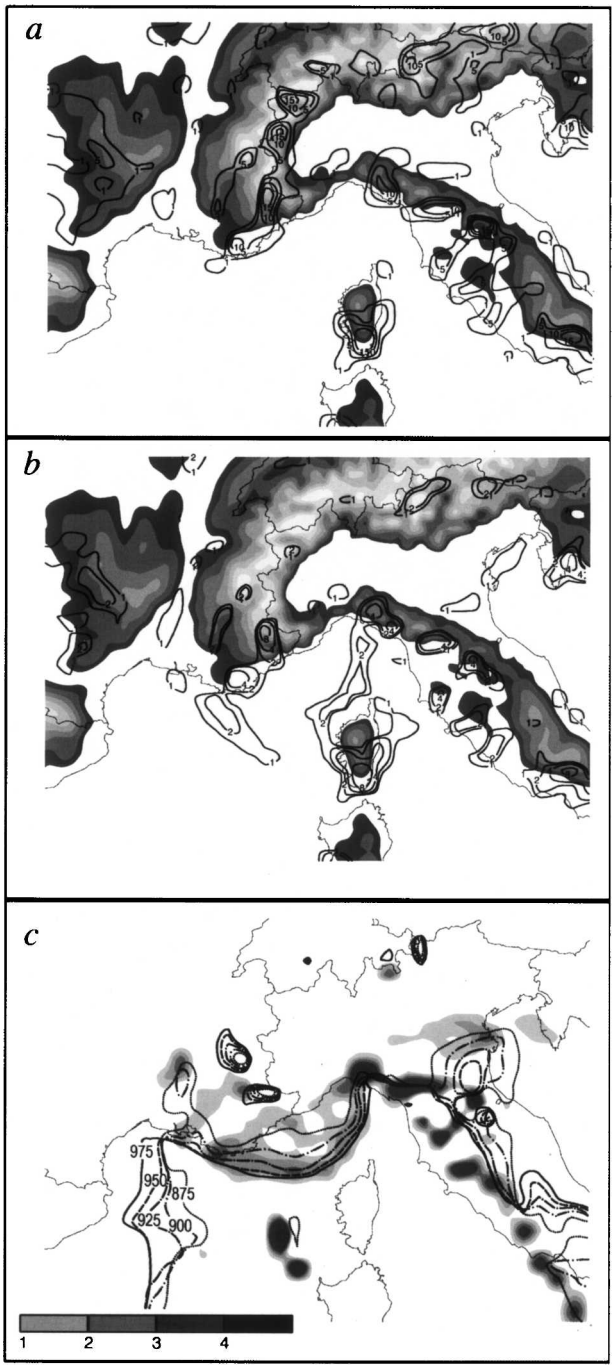

FIG. 17. MM5 15-km-resolution simulation output showing (a) terrain (shaded as in Fig. 1) and $w_{oro}q$ (contoured), (b) terrain (shaded as in Fig. 1) and wq at $\sigma = 0.995$ (contoured), and (c) height of $\theta_e = 310$ K (hPa; contoured) and $w_{eff}q$ (shaded as in legend) at 10/21/0600. Units of $w_{oro}q$, wq, and $w_{eff}q$ are 10^{-4} m g kg^{-1} s^{-1}.

Sea before it could reach the upslopes of the Alps, as hypothesized by BS03.

The cross section shown in Fig. 14, the trajectory analysis shown in Fig. 15a, and the low-level vertical ascent (Fig. 15b) suggest that lifting by the effective mountain may have provided the primary forcing for convective development over the Ligurian Sea. Furthermore, the Froude number analysis presented above reveals that convection and heavy precipitation were favored along the leading edge of the effective mountain. Taking these points into consideration, it seems that an analysis of the orographic moisture flux associated only with the effective mountain would shed some light on whether the effective mountain was the primary source of convection over the Ligurian Sea.

A similar formulation to that used for $w_{oro}q$ can be applied to the effective mountain if $h(x, y)$ is replaced by the height of the effective terrain, which is assumed to be the height of the $\theta_e = 310 \pm 10$ K contour. It is possible to use potential temperature (θ; not shown) rather than θ_e to identify the boundary of the effective mountain. These two fields show very good agreement on the location of the leading edge and height of the effective mountain; hence, the choice of θ_e for use in identifying the boundary of the effective mountain is more or less one of author preference in this case. The orographic moisture flux due to the effective mountain is referred to as $w_{eff}q$. The results of this calculation are shown in Fig. 17c. An arc-shaped pattern over the Ligurian Sea, consistent with that in Figs. 12d, 15a, and 15b, is clearly visible in the $w_{eff}q$ analysis. The results of the calculation of $w_{eff}q$ agree with our hypothesis that the cool, stable layer behaved as an effective mountain and that the lifting associated with this effective mountain is, indeed, the primary forcing of convection over the Ligurian Sea.

4. Maintenance of the stable layer

The wind vectors in Fig. 14 show that the southerly wind impinging on the stable layer was significantly stronger than the opposing northerly wind in the stable layer. Yet, the stable layer was not eroded by the southerly flow, suggesting there was some competing process that acted to maintain the strength of the stable layer. Wolyn and McKee (1989) found that for a deep stable layer ensconced in a valley in Utah, the differential advection of warmer, less stable air upon a relatively cooler, more stable air mass was the primary process leading to the stagnation of the cold air in the valley. We hypothesize that during IOP-8, the cool, stable layer over the Po Valley and Ligurian Coast was maintained by differential advection of warmer, less stable air from the Mediterranean Sea over the top of cooler, more stable air entering the Po Valley from the east.

Figure 18a shows a trajectory analysis of parcels near Milan both beneath (at 900 hPa) and above the inversion (at 750 hPa) and CAPE from the CNTL simula-

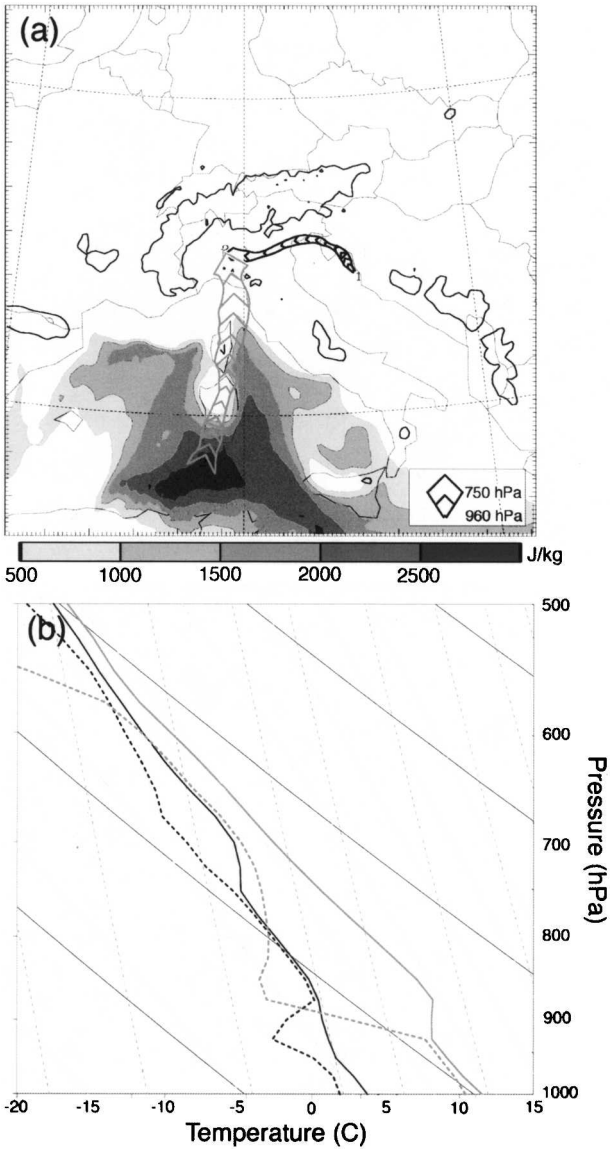

FIG. 18. MM5 15-km-resolution simulation output showing (a) backward trajectory analysis (starting at 10/21/0600 and ending at 10/21/1500 UTC) from Milan at 750 hPa (gray ribbon) and at 900 hPa (black ribbon) and CAPE (shaded as in legend at bottom of panel). Again, the width of the ribbon denotes the height of the parcel (see legend in lower right). (b) Soundings from Zadar, Croatia (black), and Cagliari (gray) at 10/21/1500 UTC.

tion. The trajectory analysis was started at 10/21/0600 and integrated backward in time to 10/20/1500. Consider the trajectory of the parcel that ended up beneath the inversion (indicated by the black ribbon in Fig. 18a). This parcel originated over the Adriatic Sea and moved northwestward. Along the foothills of the eastern flank of the Alps, the parcel was deflected westward and traveled into the Po Valley. This is consistent with the motion described by Rotunno and Ferretti (2001). The origin of this lower trajectory is roughly near Zadar, Croatia. Figure 18b shows the sounding at Zadar at 10/20/1500, which is characterized by very low CAPE (almost 0 J kg^{-1}). The lowest 150-hPa layer of this sounding was fairly stable with a moist Brunt–Väisälä frequency of 1.5×10^{-2} s^{-1}. The moist Froude number for this sounding, based on a mountain height of 2 km, is 0.24, which is significantly less than the critical moist Froude number proposed by Chen and Lin (2005a), thus implying that the lowest 150 hPa of this sounding belonged in the blocked or flow-around regime.

The trajectory above the inversion (indicated by the gray ribbon in Fig. 18a) shows that the air parcel above the inversion originated over the Mediterranean Sea at a height of about 750 hPa. The origin of this trajectory, which is located just south of Cagliari, is characterized by relatively high CAPE (over 2500 J kg^{-1}). The Cagliari sounding at 10/20/1500 is shown in Fig. 18b. This sounding is considerably warmer than the Zadar sounding. The layer between 800 and 700 hPa has an N_w of 8.1×10^3 s^{-1}, which is significantly less than the N_w for the Zadar sounding. This differential advection of a warmer, less stable air mass on top of a cooler, more stable air mass is discernible in the soundings at Milan, as discussed in section 2a.

An analysis of the source regions for the air parcels both above and beneath the inversion at Milan at different times reveals there was a persistent advection of an air mass of lower stability from the Mediterranean Sea over the top of an air mass of higher stability entering the Po Valley from the east. Such a configuration is not favorable for mixing and helps explain why the stable layer during IOP-8 was persistent for such an extended period of time and is consistent with the maintenance mechanism put forth by Wolyn and McKee (1989). In addition to the above differential advection mechanism, the Ligurian Apennines did play a secondary role in contributing to the maintenance of the cool, stable layer, as revealed and discussed in the NOAP simulation (Fig. 16).

5. Conclusions

In this research, we have examined the blocking effect of the cool, stable layer over the Po Valley during MAP IOP-8 on the formation of convection over the Ligurian Sea. Investigation of the MAP reanalysis data suggests that the stable layer in this event was strong, quasi-stationary, and protruded well into the northern Ligurian Sea. Along the leading edge of this stable layer, lightning and satellite data suggest there was deep convection. Numerical simulations using the PSU–NCAR MM5 were performed to assess, on a finer

temporal and spatial scale, what the dynamical impacts of the stable layer were on the formation of convection over the Ligurian Sea. The model-simulated synoptic-scale evolution of IOP-8 compared reasonably well with the reanalysis data, showing an upper-level jet positioned over the Po Valley such that the jet entrance region was over the northern Ligurian Sea associated with a deepening upper-level wave, a low-level, cool, dry air mass in the Po Valley that extended into the Ligurian Sea, and a moderately strong low-level jet that impinged on the cool, stable layer. The timing of model-simulated convection also appears to have been well captured. Comparison of model-simulated cloud-top temperatures with satellite-derived cloud-top temperatures shows that episodes of deep convection occurred approximately at the same times and locations in both the observations and in the model. Additional comparison of radar reflectivity, lightning strike analyses, and accumulated precipitation shows that the simulated convective activities are reasonably close to those in the observations. Final evidence that the model simulation adequately captured the pertinent thermodynamic characteristics of IOP-8 was garnered through comparison of observed soundings with model-simulated soundings.

Inspection of model-simulated θ_e, convergence, and ω fields and trajectory analyses reveals that the stable layer may have behaved as an effective mountain to the incoming southerly flow. The simulated stable layer was present several hours before the onset of convection, extending southward from the Alps over the Ligurian Sea with its leading edge positioned about 100 km upstream of the Apennines. Vertical cross sections show the southerly winds being lifted up and over the effective mountain, as though being lifted over terrain. Calculation of the orographic moisture flux for the effective mountain ($w_{\text{eff}}q$) shows that the leading edge of the effective mountain was characterized by large values in $w_{\text{eff}}q$, indicating favorable ingredients for producing a convective system and heavy rainfall there. Analysis of cross sections of the cold dome shows that there were two convective systems produced along the slope of the cold dome: one along the leading edge of the effective mountain and the other slightly south of and above the Ligurian Apennines, where the top of the cold dome intersected the level of free convection. This location and the leading edge of the cold dome were characterized by maxima of precipitation. The argument that the cold dome behaved as an effective mountain is further evidenced by the trajectory analysis, in which incoming air parcels from the Ligurian Sea were abruptly lifted by the stable layer, and by the surface convergence field, in which an arc shape was formed that is consistent in position with the leading edge of the effective mountain.

A sensitivity experiment where a portion of the Apennines along the Ligurian Coast was removed revealed only marginal decreases in the depth of the cold dome and in the strength of the inversion at the top of the cold dome. This further supports the notion that the stable layer acted as an effective mountain. In this same experiment, it was noted that the surface temperature gradient at the leading edge of the cold dome was stronger than in the CNTL simulation, suggesting the Apennines acted to partially block the southward advancement of the stable layer. However, a trajectory and sounding analysis of parcels within the stable layer, versus those above the inversion, reveals that there was a continued advection of relatively stable air into the Po Valley at low levels and advection of less stable air atop this layer. This advection of differing stability and temperature characteristics appears to have acted to inhibit mixing within the Po Valley, leading to stagnant conditions at low levels. In other words, the maintenance of the stable layer is explained by the differential advection of two air masses with different characteristics. The Ligurian Apennines made a secondary contribution to the stagnation of the cool air in the Po Valley by partially blocking this air mass from exiting the valley to the south.

This research has provided some insight on the dynamical impacts of the stable layer on the formation of convection during IOP-8, yet some questions still remain. Although the above-mentioned analyses do shed some light on why the stable layer during IOP-8 remained stagnant throughout the duration of the IOP, a deeper probe into the factors leading to the formation of the stable layer, and those that led to the ultimate demise of it, have not been addressed. Further examination of this topic is currently being addressed. This case is characterized by baroclinic forcing. It is unclear to what extent the upper-level divergence acted to enhance the low-level ascent. However, there is evidence in the idealized IOP-8 simulations of Reeves and Lin (2004) that suggests that lifting by the effective mountain alone was sufficient to generate significant upward motion. The relative importance of the baroclinic forcing and the orographically forced convergence on the development of precipitation over the Ligurian Sea will be addressed in a separate study. These two effects may be differentiated by performing a sensitivity test with all the mountains in the domain and/or with the western Alps removed. Such an experiment will also help us to understand what forcing is responsible for the formation of the broad, deep region of ascent upstream of and above the stable layer (Fig. 14).

One final topic that requires additional investigation is the notion of the effective mountain. The hypothesis that the stable layer behaved in the same sense as terrain is currently being pursued from a theoretical perspective by performing idealized numerical simulations.

Acknowledgments. This research is supported by NSF Grants ATM-0096876 and ATM-0344237. Discussions with L. Carey, S. Medina, C. Schär, F. Semazzi, J. Stein, and R. Rotunno, and the research results presented by other MAP colleagues, are highly appreciated. Some computing was performed on the supercomputers at North Carolina Supercomputer Center and North Carolina State University HPC. We thank Christoph Frei, Institute for Atmospheric and Climate Science in Zurich, Switzerland, for the objective rain gauge analyses and the anonymous reviewers for their constructive comments.

REFERENCES

Alpert, P., 1986: Mesoscale indexing of the distribution of orographic precipitation over high mountains. *J. Climate Appl. Meteor.,* **25,** 532–545.

Asencio, N., J. Stein, M. Chong, and F. Gheusi, 2003: Analysis and simulation of local and regional conditions for the rainfall over the Lago Maggiore Target Area during MAP IOP 2b. *Quart. J. Roy. Meteor. Soc.,* **129,** 565–586.

Betts, A. K., and M. J. Miller, 1993: The Betts–Miller scheme. *The Representation of Cumulus Convection in Numerical Models, Meteor. Monogr.,* No. 46, Amer. Meteor. Soc., 107–121.

Binder, P., and C. Schär, Eds., 1996: MAP design proposal. MeteoSwiss, 75 pp. [Available from the MAP Programme Office, MeteoSwiss, CH-8044, Zurich, Switzerland.]

Blackadar, A. K., 1979: High resolution models of the planetary boundary layer. *Adv. Environ. Sci. Eng.,* **1,** 50–85.

Bougeault, P., and Coauthors, 2001: The MAP special observing period. *Bull. Amer. Meteor. Soc.,* **82,** 433–462.

Bousquet, O., and B. F. Smull, 2003: Observations and impacts of upstream blocking during a widespread orographic precipitation event. *Quart. J. Roy. Meteor. Soc.,* **129,** 391–410.

Buzzi, A., N. Tartaglione, and P. Marguzzi, 1998: Numerical simulations of the 1994 Piedmont flood: Role of orography and moist processes. *Mon. Wea. Rev.,* **126,** 2369–2383.

Chen, S. H., and Y.-L. Lin, 2005a: Orographic effects on a conditionally unstable flow over an idealized three-dimensional mesoscale mountain. *Meteor. Atmos. Phys.,* **88,** 1–21.

——, and ——, 2005b: Effects of moist Froude number and CAPE on a conditionally unstable flow over a mesoscale mountain. *J. Atmos. Sci.,* **62,** 331–350.

Chu, C.-M., and Y.-L. Lin, 2000: Effects of orography on the generation and propagation of mesoscale convective systems in a two-dimensional conditionally unstable flow. *J. Atmos. Sci.,* **57,** 3817–3837.

Doswell, C. A., III, R. Romero, and S. Alonso, 1998: A diagnostic study of three heavy precipitation episodes in the western Mediterranean region. *Wea. Forecasting,* **13,** 560–581.

Dudhia, J., 1993: A nonhydrostatic version of the Penn State–NCAR Mesoscale Model: Validation tests and simulation of an Atlantic cyclone and cold front. *Mon. Wea. Rev.,* **121,** 1493–1513.

Frei, C., and E. Häller, 2001: Mesoscale precipitation analysis from MAP SOP rain-gauge data. *MAP Newsletter,* No. 15, MeteoSwiss, Zurich, Switzerland, 257–260.

Gheusi, F., and J. Stein, 2003: Small-scale rainfall mechanisms for an idealized convective southerly flow over the Alps. *Quart. J. Roy. Meteor. Soc.,* **129,** 1819–1840.

Grell, G. A., 1993: Prognostic evaluation of assumptions used by cumulus parameterizations. *Mon. Wea. Rev.,* **121,** 764–787.

Lin, Y.-L., R. D. Farley, and H. D. Orville, 1983: Bulk parameterization of the snow field in a cloud model. *J. Climate Appl. Meteor.,* **22,** 40–63.

——, S. Chiao, T.-A. Wang, M. L. Kaplan, and R. P. Weglarz, 2001: Some common ingredients for heavy orographic rainfall and their potential application for prediction. *Wea. Forecasting,* **16,** 633–660.

Medina, S., and R. A. Houze, 2003: Air motions and precipitation growth in Alpine storms. *Quart. J. Roy. Meteor. Soc.,* **129,** 345–372.

Neiman, P. J., F. M. Ralph, A. B. White, D. E. Kingsmill, and P. O. G. Persson, 2002: The statistical relationship between upslope flow and rainfall in California's coastal mountains: Observations during CALJET. *Mon. Wea. Rev.,* **130,** 1468–1492.

Reeves, H. D., and Y.-L. Lin, 2004: Effects of diabatic cooling on the formation of convective system upstream of the Apennines during MAP IOP-8. Preprints, *11th Conf. on Mountain Meteorology,* Bartlett, NH, Amer. Meteor. Soc., CD-ROM, 13.1.

Rottman, J. W., and R. B. Smith, 1989: A laboratory model of severe downslope winds. *Tellus,* **41A,** 401–415.

Rotunno, R., and R. Ferretti, 2001: Mechanisms of intense Alpine rainfall. *J. Atmos. Sci.,* **58,** 1732–1749.

——, and ——, 2003: Orographic effects on rainfall in MAP cases IOP2B and IOP8. *Quart. J. Roy. Meteor. Soc.,* **129,** 373–390.

Smith, R. B., 1979: The influence of mountains on the atmosphere. *Advances in Geophysics,* Vol. 21, Academic Press, 87–230.

——, 1985: On severe downslope winds. *J. Atmos. Sci.,* **42,** 2597–2603.

Stein, J., 2004: Exploration of some convective regimes over the Alpine orography. *Quart. J. Roy. Meteor. Soc.,* **130,** 481–502.

Tao, W.-K., and J. Simpson, 1993: Goddard Cumulus Ensemble Model. Part I. *Terr. Atmos. Oceanic Sci.,* **4,** 35–72.

Tripoli, G. J., G. Panegrossi, A. Mugnai, S. Dietrich, and E. Smith, 2000: Orographically induced flash floods on the northern Italian coast. Preprints, *9th Conf. on Mountain Meteorology,* Aspen, CO, Amer. Meteor. Soc., 336–339.

Van Tuyl, A. H., and J. A. Young, 1982: Numerical simulation of nonlinear jet streak adjustment. *Mon. Wea. Rev.,* **110,** 2038–2054.

Wolyn, P. G., and T. B. McKee, 1989: Deep stable layers in the intermountain western United States. *Mon. Wea. Rev.,* **117,** 461–472.

Zängl, G., 2003: The impact of upstream blocking, drainage flow and the geostrophic pressure gradient on the persistence of cold pools. *Quart. J. Roy. Meteor. Soc.,* **129,** 117–137.